PROCEEDINGS OF THE ROYAL SOCIETY A MATHEMATICAL, PHYSICAL & ENGINEERING SCIENCES

# Particle Behaviour in Shear and Electric Fields. I. Deformation and Burst of Fluid Drops

R. S. Allan and S. G. Mason

*Proc. R. Soc. Lond. A* 1962 **267**, 45-61
doi: 10.1098/rspa.1962.0082

# Particle behaviour in shear and electric fields
# I. Deformation and burst of fluid drops

By R. S. Allan and S. G. Mason

*Department of Chemistry, McGill University, and*
*Pulp and Paper Research Institute of Canada, Montreal, Canada*

(*Communicated by L. Marion, F.R.S.—Received* 8 *August* 1961)

The deformation and burst of liquid drops suspended in liquid dielectrics in an electric field were measured. At low electrical fields, the deformation of conducting drops into prolate spheroids showed good quantitative agreement with theoretical equations based on electrostatic theory. Dielectric drops exhibited appreciable deviation from the theory, especially in a number of systems when oblate spheroids were formed. The mode of electrical burst was found to show considerable variation with the electrical properties of the systems.

The deformation, orientation and burst under the combined action of shear and electric fields were also studied and found to agree with a theory based upon a superposition of electric- and shear-deformation forces. The mode of break-up was found to depend on the ratio of the velocity gradient to the electric field strength, on the interfacial tension, and on the ratios of dielectric constants and of viscosities of the two liquids.

## 1. Introduction

The deformation and burst of liquid drops (phase 1) suspended in another liquid (phase 2) in Couette shear flow have been discussed by Taylor (1934) and by Rumscheidt & Mason (1961). The theoretical equations developed by Taylor and by Cerf (1951) for deformation and orientation were confirmed experimentally in a large number of liquid pairs. Three classes of drop behaviour at high deformations were described and shown to depend upon the ratio of the viscosities of the two liquid pairs.

This paper describes a theoretical and experimental study of the effects of electric fields and of combined electric and shear fields upon drop deformation and burst as an extension of a few exploratory experiments (Rumscheidt & Mason 1961) and of a previous investigation (Allan & Mason 1962*a*) on the coalescence of colliding pairs of liquid drops. Apart from brief investigations of electrical dispersion of liquid threads emerging from a capillary (Zeleny 1917; Vonnegut & Neubauer 1952; Drozin 1955; Nawab & Mason 1958), the bursting of soap bubbles in electric fields (Wilson & Taylor 1925), and the deformation of liquid drops in uniform electric fields (O'Konski & Thacher 1953; O'Konski & Gunther 1955; O'Konski & Harris 1957), little attention appears to have been directed to this subject.

In the theoretical section which follows, equations are derived for deformation and burst of drops as functions of the electric and shear field parameters, and of the viscosity ratio, and the ratio of the dielectric constants of the two liquid pairs. Most of these equations have been tested experimentally over a wide range of conditions.

## 2. Theoretical

### (a) *Deformation in an electric field*

The deformation of an incompressible fluid drop by an electric field results from electrical stresses developed on the interface which in the equilibrium position are balanced by interfacial tension forces. The analysis presented here is limited to small deformations, i.e. to drops which are very nearly spherical, and differs somewhat from the treatment of O'Konski & Thacher (1953) although it leads to similar results.

The potentials inside $V_1$ and outside $V_2$ a sphere of radius $b$ in a macroscopically uniform field of strength $E_0$ directed along the $Y$ axis of a rectangular co-ordinate system are given by the well-known electrostatic equations

$$V_1 = \left(\frac{3}{q+2}\right) E_0 R\cos\phi, \tag{1}$$

and

$$V_2 = \left[1 - \frac{b^3}{R^3}\left(\frac{q-1}{q+2}\right)\right] E_0 R\cos\phi, \tag{2}$$

where $(R, \phi)$ are the polar co-ordinates with the sphere centred at the origin, $\phi$ is the angle between the radius vector and the $Y$ axis (figure 1) and $q$ is the ratio of the dielectric constant of the drop ($K_1$) to that of the suspending medium ($K_2$). The corresponding tangential and normal components of the local field strengths on the outside of the sphere are therefore (Harnwell 1949, p. 45)

$$E_{t,2} = \frac{1}{b}\left(\frac{\partial V_2}{\partial \phi}\right)_{R=b} = -\left(\frac{3}{q+2}\right) E_0 \sin\phi, \tag{3}$$

$$E_{n,2} = \left(\frac{\partial V_2}{\partial R}\right)_{R=b} = \left(\frac{3q}{q+2}\right) E_0 \cos\phi. \tag{4}$$

The normal electrical stress ($f_n$) acting outwards on the interface is (Smythe 1953)

$$f_n = \frac{K_1 - K_2}{8\pi K_2}\left[\frac{\Delta_{t,2}^2}{K_2} + \frac{\Delta_{n,2}^2}{K_1}\right] \tag{5}$$

where the electric displacements

$$\Delta_{t,2} = K_2 E_{t,2}, \tag{6a}$$

and

$$\Delta_{n,2} = K_2 E_{n,2}. \tag{6b}$$

On combining (3) to (6) and simplifying, we obtain

$$f_n = \beta_e[\mu + \cos 2\phi], \tag{7}$$

where

$$\beta_e = \frac{9K_2 E_0^2 (q-1)^2}{16\pi(q+2)^2} \tag{8}$$

and

$$\mu = (q+1)/(q-1). \tag{9}$$

To balance $f_n$ changes in curvature of the interface must satisfy Laplace's equation in the form

$$\gamma(b_1^{-1} + b_2^{-1}) = (p_i - p_0) + f_n, \tag{10}$$

where $b_1$ and $b_2$ are principal radii of curvature at any point on the interface, $p_i$ and $p_0$ are the (constant) hydrostatic pressures inside and outside the drop and $\gamma$ is the interfacial tension.

Substituting for $f_n$ in (10) and rearranging we have

$$\gamma(b_1^{-1}+b_2^{-1}) = \beta_e \cos 2\phi + \text{constant}. \tag{11}$$

Thus we are required to find the shape of a nearly spherical drop in which the variation of the curvature is proportional to $\cos 2\phi$. This is similar to the problem considered by Taylor (1934) for the deformation of a drop in a field of Couette flow given by

$$u = Gy, \quad v = w = 0, \tag{12}$$

where $u$, $v$ and $w$ are the velocity components along the $X$, $Y$ and $Z$ axes of the shear field and $G$ is the velocity gradient. In this case, the curvature is given by

$$\gamma(b_1^{-1}+b_2^{-1}) = \beta_s \cos 2\phi' + \text{constant}, \tag{13}$$

$$\text{where} \quad \phi' = (\phi - \tfrac{1}{4}\pi), \quad \beta_s = 4\eta_2 G f(p) \quad \text{and} \quad f(p) = (19p+16)/(16p+16) \tag{14}$$

and $p = \eta_1/\eta_2$ is the ratio of the viscosity of the drop to that of the medium.

Taylor showed that (13) is satisfied for small deformations $D > 0$ by an approximately ellipsoidal particle whose $z = 0$ cross-section is given by the polar equation

$$R = b[1 + D_s \cos 2\phi'], \tag{15}$$

$$\text{where the deformation,} \qquad D_s = b\beta_s/4\gamma. \tag{16}$$

Comparing (11) with (13), it follows by analogy that the electrical deformation is given by replacing $\phi'$ by $\phi$, and $D_s$ by

$$D_e = \frac{b\beta_e}{4\gamma} = \frac{9bK_2E_0^2(q-1)^2}{64\pi\gamma(q+2)^2} \tag{17}$$

in (15).

The particle thus becomes a prolate spheroid (figure 1) with an axis of revolution $L$ oriented along $\phi_m$ (or in Couette flow $\phi'_m$) $= 0$ and of equatorial diameter $B$ given by

$$D = (L-B)/(L+B). \tag{18}$$

It should be noted that making the drop a conductor imposes the boundary condition that the sphere has an equipotential surface. Analytically this is equivalent to setting $q = \infty$ in (8) and (17) which then reduce to

$$(\beta_e)_{q=\infty} = \frac{9K_2E_0^2}{16\pi}, \quad (D_e)_{q=\infty} = \frac{9bK_2E_0^2}{64\pi\gamma}. \tag{19}$$

For small values of the eccentricity $e$, $D = \frac{1}{4}e^2$ and (17) and (19) become identical with those of O'Konski & Thacher (1953) derived from the energy equations instead of the force equations employed above.

### (*b*) *Electrical burst*

As the field $E_0$ is increased, the stresses on the drop increase until the surface tension can no longer contain them and the drop bursts. The field at which this will just occur can be estimated in the same way as for Couette flow (Taylor 1934; Rumscheidt & Mason 1961).

The total electrical force acting along the $Y$ axis of the hemisphere on each side of the $y = 0$ equator is

$$F_y = \int_0^{\frac{1}{2}\pi} 2\pi b^2 f_n \cos\phi \sin\phi \, d\phi. \tag{20}$$

$F_y$ increases with the field until a critical value $E_{0,B}$ is reached at which $F_y$ pulling the drop apart just balances the interfacial tension forces holding the drop together, i.e. when $F_y = 2\pi b\gamma$.

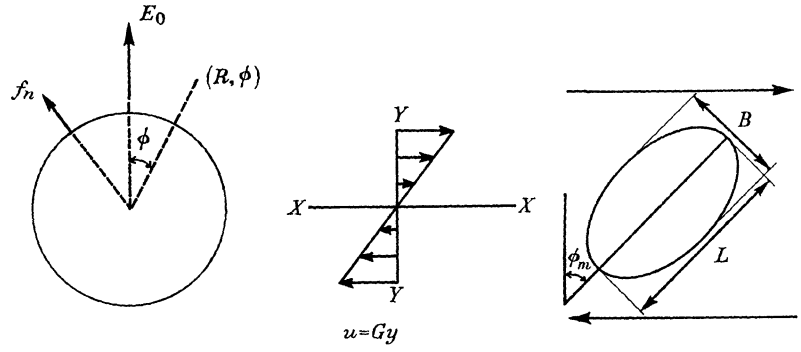


FIGURE 1. Parameters used in electric and shear deformation equations. The equatorial planes ($z = 0$) of the drops are shown in the undeformed state ($a$) and the deformed state ($b$).

Under these conditions it follows from (7) and (20) that this occurs when

$$\beta_{e,B} = 2\gamma/\mu b \tag{21}$$

from which it follows that

$$D_{e,B} = 1/2\mu \tag{22}$$

and

$$E^2_{0,B} = \frac{32\pi\gamma(q+2)^2}{9bK_2\mu(q-1)^2}. \tag{23}$$

It follows from (22) that when $q = \infty$ ($\mu = 1$), the deformation at burst is $\frac{1}{2}$. This is the value predicted for shear burst (Rumscheidt & Mason 1961; Taylor 1934) which in the notation used here corresponds to

$$\beta_{s,B} = 2\gamma/b. \tag{24}$$

As will be seen later, (22) to (24) are only rough approximations, since they are based on a spherical model which also neglects the internal pressure $p_i$ whereas since $D_B > 0$, the drops are ellipsoidal. For simplicity, therefore, we will write $D_B = \frac{1}{2}$ for both fields.

### (c) *Charge separation at burst*

It is of interest to calculate the charge accumulation on the drops following burst. It is assumed that $q = \infty$, and that the initially neutral drop breaks into two halves each bearing the total induced charge on each hemisphere bounded by the $y = 0$ plane (figure 1).

From elementary electrostatics the charge density $\sigma$ on the primary drop is given by

$$\sigma = (3K_2/4\pi)\, E_0 \cos\phi, \tag{25}$$

Integrating over each hemisphere yields the total charge $Q$ per hemisphere at burst

$$Q = \pm \tfrac{3}{4} K_2 b^2 E_{0,B}. \tag{26}$$

This relationship will be used in a future publication.

### (*d*) *Deformation and burst in combined electric and shear fields*

We assume that when the two fields are combined the normal stresses created at the interface are additive. From (10), (11) and (13), it follows that

$$\gamma(b_1^{-1} + b_2^{-1})_{e+s} = \beta_e \cos 2\phi + \beta_s \sin 2\phi + \text{constant} \tag{27}$$

$$= \beta_n \cos 2(\phi - \phi_m) + \text{constant}, \tag{28}$$

where

$$\phi_m = \tfrac{1}{2} \tan^{-1}(\beta_s/\beta_e) \tag{29}$$

and

$$\beta_n = (\beta_e^2 + \beta_e^2)^{\frac{1}{2}}. \tag{30}$$

By analogy with (15), the drop assumes an ellipsoidal shape with a net deformation,

$$D_n = (D_e^2 + D_s^2)^{\frac{1}{2}} \tag{31}$$

oriented at the angle $\phi_m$ given by

$$\phi_m = \tfrac{1}{2} \tan^{-1}(D_s/D_e). \tag{32}$$

It should be noted that (31) and (32) satisfy the relations previously derived for $E_0 = 0$ and $G = 0$.

Similarly, at burst, $D_{n,B} = \frac{1}{2}$ *approx.*

The analysis leading to (31) and (32) is based on the assumption that the principal deformation in shear alone occurs at $\phi_m = \frac{1}{4}\pi$.

Owing to drop rotation, however, which makes the deformation at a point on the rotating drop subject to relaxation effects, this orientation applies strictly only at $G = 0$. At finite gradients, a better approximation is given by Cerf's equation (1951) which has been confirmed experimentally (Rumscheidt & Mason 1961).

In this case, the deformation equation is

$$\gamma(b_1^{-1} + b_2^{-1})_s = \beta_s \sin 2(\phi - \psi_d) + \text{constant}, \tag{33}$$

where

$$\psi_d = (1 + \tfrac{2}{5}p)\, D_s. \tag{34}$$

Equation (33) predicts a drop orientation at $\phi_m = \psi_d + \frac{1}{4}\pi$.

Replacing the shear deformation term in (27) by (33) and proceeding as before we obtain the corrected values (indicated by primes)

$$D'_n = (D_e^2 - 2D_s D_e \sin 2\psi_d + D_s^2)^{\frac{1}{2}}, \tag{35}$$

$$\phi'_m = \tfrac{1}{2} \tan^{-1}\left[\frac{D_s \cos 2\psi_d}{D_e - D_s \sin 2\psi_d}\right]. \tag{36}$$

In the equations considered above, the electrical quantities are all expressed in electrostatic units.

## 3. Experimental methods

### (a) *Apparatus*

All experiments were performed in the Couette apparatus (Rumscheidt & Mason 1961; Bartok & Mason 1957) designed for viewing the drops along the $Z$ axis through a stereomicroscope with the use of transmitted light and heat filters.

Drop deformation is shear and electric fields was recorded photographically with a motor-driven Bolex Paillard H-16 (16 mm) cine-camera mounted directly on the stereomicroscope in combination with a beam splitter. The developed film was analyzed frame by frame by projection onto a drafting table.

An electric field was applied normal to the direction of shear flow (i.e. along the $Y$ axis of the co-ordinate system) by grounding the inner cylinder and connecting the outer (insulated) cylinder to the positive (or negative) lead of a 0 to 10 kV stabilized d.c. power supply. To obtain as high fields as possible the large inner cylinder was used, giving an annulus 1·88 cm wide. The field strength, $E_0$, expressed as volts/centimetre, was calculated on the assumption that the field was uniform across the gap. Strictly speaking, $E_0$ varied because of curvature of the Couette cylinders according to the well-known relation for a concentric cylindrical condenser

$$E_0(R) = \frac{V_a}{R \ln R_2/R_1}, \tag{37}$$

where $E_0(R)$ is the field strength at the radial distance, $R$, $R_1$ and $R_2$ are the radii of the inner and outer cylinders and $V_a$ is the potential difference across the annulus. Since $R_1 = 13{\cdot}36$ cm and $R_2 = 15{\cdot}24$ cm, $E_0(R_1)/E_0(R_2) = 1{\cdot}14$; this variation was ignored, although in several cases of burst, the increased field on the side of the drop near the inner cylinder was probably important.

To prevent excessive current leakage through the annulus the aqueous substrate used in previous work (Bartok & Mason 1957) was omitted.

The viscosity of the liquids used was measured in a thermostatically controlled ($20{\cdot}00 \pm 0{\cdot}01$ °C) rotational viscometer (Drage viscometer, A. G. Epprecht, Chemisches Institut, Zurich, Switzerland) at shear rates ranging between 4 and 125 $s^{-1}$.

The dielectric constants ($K$) and d.c. conductivities ($\kappa$) were kindly measured by Dr D. W. Davidson, National Research Council, Ottawa, with a three terminal cell of some 35 $\mu$F capacitance at frequencies ranging from 0·050 to 500 kc/s.

The room temperature was controlled at $20 \pm 1$ °C.

### (b) *Materials*

The properties of the fluid systems used are listed in table 1. Care was taken to prevent contamination of the drop interfaces by impurities. The drop diameters were between 300 and 2000 $\mu$ and were measured by a calibrated grid in the microscope. The grid was carefully alined with the axis of flow in the Couette apparatus. All the liquids were found to be Newtonian over the range of gradients employed in the viscosity measurements with the exception of CHP (sextol phthalate) which was slightly visco-elastic. To make the water drops conducting ($q = \infty$), 0·07% KCl was added.

PROCEEDINGS OF THE ROYAL SOCIETY A MATHEMATICAL, PHYSICAL & ENGINEERING SCIENCES



TABLE 1. PROPERTIES OF FLUID SYSTEMS

Temperature = 20 °C

| system no. | continuous (phase 2) | $\eta_2$ (P) | $K_2$ | $\kappa_2$ ($\Omega^{-1}$ cm$^{-1}$) | drop (phase 1) | $p$ | $q$ | $\kappa_1$ ($\Omega^{-1}$ cm$^{-1}$) | deformation[g] class in shear field |
|---|---|---|---|---|---|---|---|---|---|
| 1 | silicone oil 5000[a] | 53·3 | 2·77 | $< 3 \times 10^{-13}$ | CHP[b] | 3·8 | 2·18 | $4{\cdot}5 \times 10^{-12}$ | C |
| 2 | | | | | Pale 4[c] | 1·0 | 2·27 | $1 \times 10^{-11}$ | B 1 |
| 3 | | | | | LB—1715[d] | 0·19 | 1·93 | $3{\cdot}6 \times 10^{-11}$ | B 1 |
| 4 | | | | | water[e] | $2 \times 10^{-4}$ | $\infty$ | $1{\cdot}1 \times 10^{-3}$ | A |
| 5 | | | | | water + 0·3 % Tween 20[f] | $2 \times 10^{-4}$ | $\infty$ | $1{\cdot}1 \times 10^{-3}$ | A |
| 6 | Pale 4[c] | 53·0 | 6·30 | $1 \times 10^{-11}$ | silicone oil 60000[a] | 12 | 0·44 | $< 3 \times 10^{-13}$ | C |
| 7 | | | | | silicone oil 5000[a] | 1·0 | 0·44 | $< 3 \times 10^{-13}$ | B 1 |
| 8 | | | | | silicone oil 1000[a] | 0·19 | 0·44 | $< 3 \times 10^{-13}$ | B 1 |
| 9 | | | | | water[e] | $2 \times 10^{-4}$ | $\infty$ | $1{\cdot}1 \times 10^{-3}$ | A |
| 10 | LB 1715[d] | 10·0 | 5·33 | $3{\cdot}6 \times 10^{-11}$ | silicone oil 5000[a] | 5·3 | 0·52 | $< 3 \times 10^{-13}$ | C |
| 11 | | | | | silicone oil 1000[a] | 1·0 | 0·52 | $< 3 \times 10^{-13}$ | B 1 |
| 12 | | | | | ethylene glycol | $2 \times 10^{-2}$ | 7·02 | $1{\cdot}2 \times 10^{-6}$ | A |
| 13 | | | | | water[e] | $1 \times 10^{-3}$ | $\infty$ | $1{\cdot}1 \times 10^{-3}$ | A |

[a] Dow Corning fluid.
[b] Sextol phthalate (Howard and Sons (Canada) Ltd.).
[c] Oxidized castor oil (Baker Castor Oil Co., New York).
[d] Ucon oil (Carbide and Carbon Chemicals Co.).
[e] Distilled water containing 0·07 % KCl to make it a conductor.
[f] Polyoxyethylene sorbitan monolaurate, oil-in-water emulsifier (Atlas Powder Co.).
[g] See Rumscheidt & Mason (1961) for identification.

## 4. Experimental results

### (a) *Deformation in shear flow* ($E_0 = 0$)

The deformation of drops in a velocity gradient for the systems listed in table 1 was as previously reported (Rumscheidt & Mason 1961). At low gradients, a drop was deformed into a prolate spheroid initially alined at $\phi_m = 45°$, with both $D_s$ and $\phi_m$ increasing with $G$. As the deformation increased, three distinct modes of behaviour occurred depending on $p$ and $\gamma$ as listed in the last column of table 1. They are briefly described as follows:

(1) *Class A*. At $G > G_B$, the drop assumed a sigmoidal shape at $\phi_m > \frac{1}{4}\pi$ with pointed ends from which small fragments of phase 1 liquid were emitted. After a time at constant $G$, the volume and hence $Gb$ were reduced until the stable spheroidal shape was re-established.

(2) *Class B* 1. At $G_B$, the central portion of the drop suddenly started to extend into a cylinder with a neck in the middle which progressively thinned until two identical drops and three satellite drops were formed.

(3) *Class C*. As $G$ increased, at high values of $p$, the ellipsoidal drop reached a limiting value of deformation at $\phi_m = \frac{1}{2}\pi$.

A fourth class of break-up (*B* 2) which was not observed here, was also reported by Rumscheidt & Mason (1961). This was a variation of class *B* 1 in which when $G > G_B$, the drop became extended into a long thread which increased in length until it broke up into a large number of fine droplets.

Some typical examples showing the variation in $D_s$ and $\phi_m$ with $Gb$ for different classes of drop behaviour are given in figure 2. Tables 2 and 3 give the values of $\gamma_s$ calculated from the initial slopes of the $D_s$ curves for the systems examined, using (16) which was previously found (Rumscheidt & Mason 1961) to give good agreement with $\gamma$ determined independently by standard methods.

As previously reported (Rumscheidt & Mason 1961) and as shown in figure 2(*a*), there was deviation from (16) which was sometimes positive (curving upwards, $(\mathrm{d}^2D_s/\mathrm{d}G^2) > 0$) and sometimes negative (curving downwards, $(\mathrm{d}^2D_s/\mathrm{d}G^2) < 0$). Except at high values of $p$ (class C) where the deviation was negative, no systematic correlation of $(\mathrm{d}^2D_s/\mathrm{d}G^2)$ with system properties could be found (Rumscheidt & Mason 1961).

### (b) *Deformation in an electric field* ($G = 0$)

#### (i) *General observations*

The general behaviour of all systems listed in table 1 in an electric field was as predicted by the theory except for those systems in which $q < 1$ when the drops deformed into oblate spheroids.

As $E_0$ (and $D_e$) increased, three distinct modes of behaviour were observed depending mainly on $q$. These are illustrated in figure 3 and may be described as follows:

(1) $q = \infty$. As $E_0$ increased, $D_e$ increased, the drop remaining spheroidal until at $E_{0,B}$, it suddenly separated into two approximately equal parts with a larger number of fine droplets in between (figure 3(*a*)); the two principal daughter drops

moved apart rapidly as a result of the separation of charge. Occasionally, when the drop had moved across the annulus because of the electro-osmotic effect previously observed (Allan & Mason 1962*a*) break-up occurred from the end of the drop nearest the negative (inner) electrode. This was probably due to the field enhancement expressed by (37).

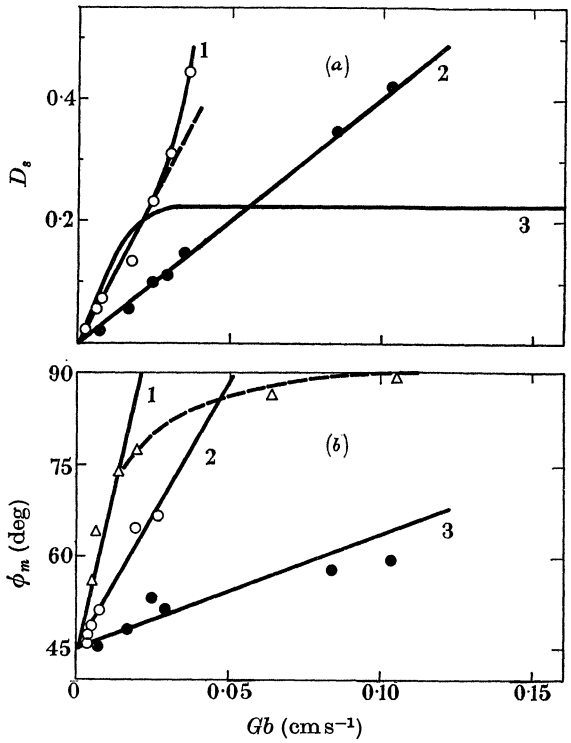


FIGURE 2. (*a*) Typical deformation curves in shear flow illustrating class A (curve 2, system 9), class B (curve 1, system 7) and class C (curve 3, system 1) deformations. (*b*) Variation of $\phi_m$ with $Gb$ for the same three systems. Curves 1, 2, and 3 correspond to systems 1, 7 and 9, respectively. Note how rapidly $\phi_m$ approaches 90° in curve 1 (class C deformation). The lines were calculated from Cerf's theory (1951) using $\gamma_s$ from the deformation curves.

TABLE 2. DROP DEFORMATION AND BREAK-UP IN ELECTRIC AND SHEAR FIELDS

$q = \infty$.

| system no. | $p$ | $\gamma_e$[a] (dynes cm$^{-1}$) | $\gamma_s$[b] (dynes cm$^{-1}$) | $\gamma_e/\gamma_s$ | $(E_0^2 b)_B$ (meas.) ($10^6$ V$^2$ cm$^{-1}$) | $(E_0^2 b)_B$[c] (calc.) ($10^6$ V$^2$ cm$^{-1}$) | $D_{e,B}$ (meas.) | $D_{s,B}$ (meas.) |
|---|---|---|---|---|---|---|---|---|
| 4 | $2 \times 10^{-4}$ | 11·8 | 13·8 | 0·86 | 1·0 | 4·3 | — | — |
| 5 | $2 \times 10^{-4}$ | 7·7 | 5·3 | 1·45 | 1·5 | 2·8 | — | — |
| 9 | $2 \times 10^{-4}$ | 9·0 | 10·7 | 0·84 | 0·4 | 1·4 | 0·16 | 0·55 |
| 13 | $1 \times 10^{-3}$ | 2·3 | 5·5 | 0·42 | 0·29 | 0·45 | 0·36 | 0·56 |
| | | | mean values | 0·89 | $\dfrac{(E_0^2 b)_B\,(\text{meas.})}{(E_0^2 b)\,(\text{calc.})} = 0{\cdot}36$ | | 0·17 | 0·54 |

*a* om (19). *b* From (16). *c* From (23) with $\gamma_e$ from (19).

After moving through a distance of 0·1 to 0·2 cm, the fragment near the positive electrode stopped and began moving in the direction of the negative electrode. This was no doubt due to negative charge leakage previously observed in silicone oil (Allan & Mason 1962*a*) with the resulting neutral drop moving in the opposite direction because of the electro-osmotic effect.

With water drops in LB-1715, there was a tendency towards pointed ends at break-up as observed for soap bubbles bursting in an electric field (Wilson & Taylor 1925).

TABLE 3. DROP DEFORMATION AND BREAK-UP IN ELECTRIC AND SHEAR FIELDS

| system no. | $p$ | $\gamma_e$[a] (dyne cm$^{-1}$) | $\gamma_s$[b] (dyne cm$^{-1}$) | $\gamma_e/\gamma_s$ | $(E_0^2 b)_B$ (meas.) ($10^6$ V$^2$ cm$^{-1}$) | $(E_0^2 b)_B$[c] (calc.) ($10^6$ V$^2$ cm$^{-1}$) | $D_{e,B}$ (meas.) | $D_{s,B}$ (meas.) |
|---|---|---|---|---|---|---|---|---|
| Systems deviating from (17) | | | | | | | | |
| $q > 1$ | | | | | | | | |
| 1 | 3·8 | 0·19 | 5·6 | 0·03 | $0{\cdot}32 \times 10^6$ | $0{\cdot}85 \times 10^6$ | 0·14 | 0·25[d] |
| 2 | 1·0 | 0·32 | 4·3 | 0·08 | $0{\cdot}54 \times 10^6$ | $1{\cdot}3 \times 10^6$ | 0·17 | 0·44 |
| 3 | 0·19 | 0·12 | 2·8 | 0·04 | $0{\cdot}21 \times 10^6$ | $0{\cdot}75 \times 10^6$ | 0·16 | 0·51 |
| 12 | 0·02 | 1·8 | 5·8 | 0·31 | $0{\cdot}29 \times 10^6$ | $0{\cdot}69 \times 10^6$ | 0·23 | 0·62 |
| | | | mean values | 0·15 | $\frac{(E_0^2 b)_B \text{ meas.}}{(E_0^2 b)_B \text{ calc.}} = 0{\cdot}38$ | | 0·18 | 0·52 |
| $q < 1$[e] | | | | | | | | |
| 6 | 12·0 | — | 5·1 | — | $2{\cdot}0 \times 10^6$ | — | −0·07 | 0·10[d] |
| 7 | 1·0 | — | 4·4 | — | $3{\cdot}7 \times 10^6$ | — | −0·16 | 0·51 |
| 8 | 0·19 | — | 4·5 | — | $1{\cdot}2 \times 10^6$ | — | −0·04 | 0·55 |
| 10 | 5·3 | — | 2·6 | — | $0{\cdot}91 \times 10^6$ | — | — | 0·28[d] |
| 11 | 1·0 | — | 3·0 | — | $1{\cdot}1 \times 10^6$ | — | — | 0·56 |

*a* From (17).
*b* From (16).
*c* From (23) with $\gamma_e$ from (17).
*d* Limiting deformation in shear field (class C deformation).
*e* These systems yielded oblate spheroids in the electric field ($D_e < 0$).

(2) $1 < q < \infty$. Again $D_e$ increased progressively, the drop remaining spheroidal until, suddenly, the end of the drop near the negative electrode was pulled out into a thin thread which moved directly towards the negative electrode (figure 3(*b*)). The same behaviour was observed when the field was reversed or when the drops were initially placed near the positive electrode; this indicates negative charge leakage (Allan & Mason 1962*a*) from the other end of the drop. With LB 1715 in silicone oil (system 3) the moving thread lashed to and fro. When $E_0$ was further increased, the other end of the drop extended into a thread which moved towards the positive electrode without breaking up. When the field was discharged, the thread broke up into a large number of small droplets as observed with class B 2 systems in a shear field (Rumscheidt & Mason 1961).

(3) $q < 1$. At $p < 1{\cdot}0$ (class B 1), the drop deformed into a sheet at $E_0 > E_{0,B}$ which was initially alined in the $ZX$ plane (figure 3(*c*)). The flattened drop then folded over and twisted until it was no longer co-planar eventually breaking up unevenly. Class C materials flattened and folded over without burst up to $E_0 = 5300$ V/cm. In contrast to previous observations (Allan & Mason 1962*a*) a definite drift to the positive electrode was always observed in these cases.

(ii) *Variation of $D_e$*

The variation of $D_e$ with $E_0$ was measured for all the systems listed in table 1. Some typical examples are given in figure 4. Table 2 shows the values of $\gamma_e$ calculated from the initial slopes of the $D_e$ curves from (17) and (19) for systems where $q = \infty$. Good agreement was observed with the corresponding values of $\gamma_s$ calculated from (16) the mean value of $\gamma_e/\gamma_s$ being 0·89. Table 3 gives the values of

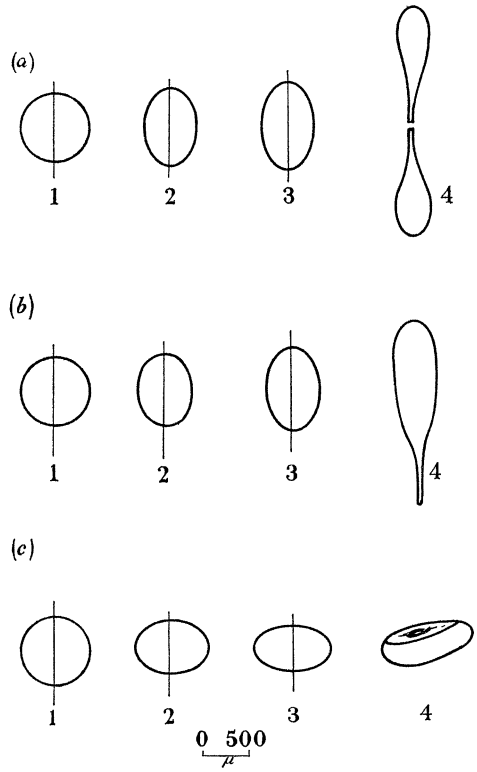


FIGURE 3. Tracings from typical photographs of drops in an electric field showing the change in $D_e$ with increasing $E_0$ up to break-up. (*a*) $q = \infty$ (system 13). The drop in picture 4 separated into two halves with a large number of fine droplets in between at $(E_0^2 b) = 2{\cdot}9 \times 10^5\,\mathrm{V^2\,cm^{-1}}$. (*b*) $1 < q < \infty$ (system 2). The drops were drawn out into threads starting from the end nearest the negative electrode (as shown) followed by extension of the other end to the positive electrode at $(E_0^2 b) = 5{\cdot}4 \times 10^5\,\mathrm{V^2\,cm^{-1}}$. (*c*) $q < 1$ (system 7). The drops were flattened into a sheet initially in the $XZ$ plane (picture 4), which then folded over until it was no longer co-planar. The flattened drop eventually broke up unevenly at $(E_0^2 b) = 3{\cdot}7 \times 10^6\,\mathrm{V^2\,cm^{-1}}$.

$\gamma_e$ calculated from (17) for systems where $1 < q < \infty$. It can be seen that the $\gamma_e$ values are very much lower than the corresponding $\gamma_s$ values, indicating a deviation from (17). This is discussed later. Except when $q = \infty$, the variation of $D_e$ with $E_0^2 b$ was linear up to electrical burst, including the systems yielding oblate spheroids corresponding to $D_e < 0$.

(iii) *Drop break-up*

The measured values of $(E_0^2 b)_B$ and those calculated from (23) for drops with $D_e > 0$ using the measured values of $\gamma_e$, are given in tables 2 and 3, along with the measured values of $D_{e,B}$ and $D_{s,B}$. It can be seen that, in all cases, the measured values of $(E_0^2 b)_B$ are lower than the calculated values. This may be expected since the theory assumes that the drops remain spherical in an electric field, and also since there is an increase in the electrostatic force due to field enhancement as the drops extend towards the electrodes. The measured values of $D_{e,B}$ were all lower than the predicted value (22), whereas the mean value of $D_{s,B}$ (tables 2 and 3) was 0·53 in accordance with previous findings (Rumscheidt & Mason 1961).

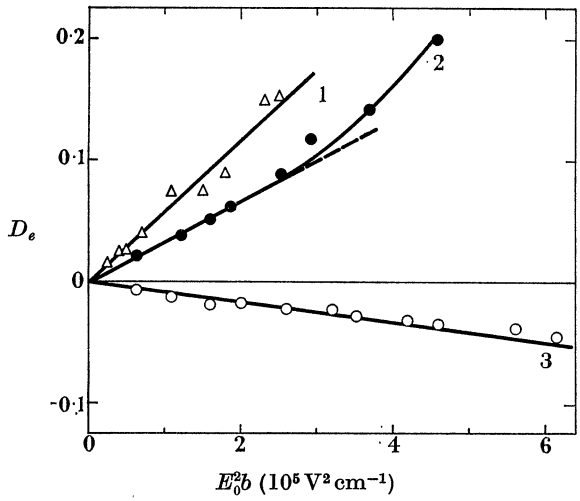


FIGURE 4. Deformation in an electric field. Curves 1, 2 and 3 correspond to system 1 ($1 < q < \infty$), 9 ($q = \infty$) and 7 ($q < 1$), respectively. In the first two cases the drops deformed into prolate spheroids ($D > 0$) and in the third case, the drop deformed into an oblate ($D < 0$) spheroid. In all cases, the axis of revolution was in the direction of the electric field.

### (c) *Deformation in a combined shear and electric field*

(i) *Net deformation*

Typical examples showing the measured and calculated values of $D_n$ are given in figure 5. The agreement is seen to be excellent. The mean values of $D_n$ (meas.)/$D_n$ (calc.) for all the systems examined are given in table 4 for $Gb = 0{\cdot}004$ to $0{\cdot}15\ \mathrm{s}^{-1}$ and $(E_0^2 b) = 0{\cdot}4 \times 10^5$ to $10 \times 10^5$ V/cm. The overall mean is $1{\cdot}00 \pm 0{\cdot}07$. The values of $D_n'$ calculated from (35) were only about 5 % lower than $D_n$ calculated from (31), with an increasing deviation from the measured values as $D_n$ increased.

(ii) *Effect of an electric field on $\phi_m$*

When $q > 1$, the effect of an electric field at a constant $G$ was to decrease $\phi_m$, the effect diminishing as $G$ increased. Similarly when $q < 1$, $\phi_m$ increased as $E_0$ increased. The values of $\phi_m$ calculated from (32) deviated considerably from the measured

values, especially as $D_n$ increased. This might be expected since (32) gives a maximum value of $\phi_m = \frac{1}{4}\pi$ when $E_0 = 0$. The values of $\phi'_m$ calculated from (36) on the other hand show very good agreement with the measured values as seen in figure 6 which shows typical examples. The mean values of $\phi_m$ (meas.)/$\phi'_m$ (calc.) for all the systems examined are given in table 4. Except for systems 2 and 3 the agreement is very good with an overall mean of $1{\cdot}03 \pm 0{\cdot}07$. A deviation might be expected for these latter systems since they have already been shown to deviate from (17).

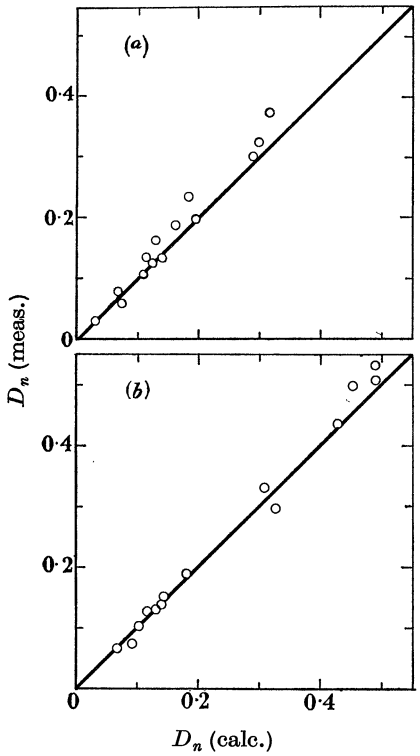


FIGURE 5

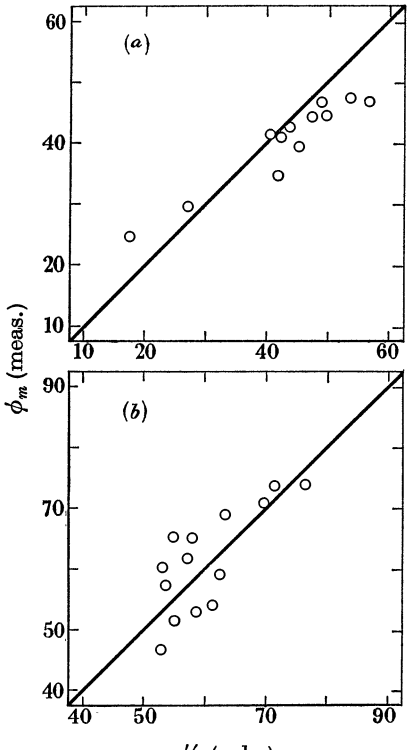


FIGURE 6

FIGURE 5. Comparison of measured and calculated values of $D_n$ for (*a*) system 9 ($q = \infty$) and (*b*) system 3 ($1 < q < \infty$). The lines are calculated from (31). The ranges of the experimental parameters were as follows:

| system | $Gb$ (cm s$^{-1}$) | $E_0^2 b$ ($10^5$ V$^2$ cm$^{-1}$) | $D_s$ | $D_e$ |
|---|---|---|---|---|
| 9 | 0·003 to 0·04 | 0·2 to 3·1 | 0·02 to 0·30 | 0·01 to 0·16 |
| 3 | 0·004 to 0·021 | 0·2 to 1·9 | 0·07 to 0·41 | 0·01 to 0·13 |

FIGURE 6. Comparison of measured and calculated values of $\phi'_m$ for (*a*) system 4 ($q = \infty$) and (*b*) system 7 ($q < 1$). The lines are calculated from (36). The ranges of the experimental parameters were as follows:

| system | $Gb$ (cm s$^{-1}$) | $E_0^2 b$ ($10^5$ V$^2$ cm$^{-1}$) | $D_s$ | $D_e$ |
|---|---|---|---|---|
| 4 | 0·005 to 0·098 | 0·3 to 4·3 | 0·02 to 0·40 | 0·01 to 0·04 |
| 7 | 0·004 to 0·027 | 1·1 to 9·7 | 0·03 to 0·31 | 0·03 to 0·40 |


PROCEEDINGS OF THE ROYAL SOCIETY A MATHEMATICAL, PHYSICAL & ENGINEERING SCIENCES

(iii) *Drop break-up in shear and electric fields*

Generally the mode of break-up in a combined shear and electric field was similar to that found with an electric field alone with modifications due to $G$.

(1) $q = \infty$. At $E_{0,B}$, deformed drops suddenly separated into two parts which moved towards the electrodes in the direction of the electric field because of charge separation and also along the axis of flow. As $Gb$ and hence $D_s$ increased, $(E_0^2 b)_B$ decreased. When $G$ was close to $G_B$, an electric field increased $D_n$ sufficiently so that break-up occurred as in a shear field alone. In other cases, because the drop had moved across the annulus as a result of the electro-osmotic effect (Allan & Mason

TABLE 4. COMPARISON OF MEASURED AND CALCULATED VALUES OF $D_n$ AND $\phi_m$

Summary table
$Gb = 0{\cdot}004$ to $0{\cdot}15\,\mathrm{s}^{-1}$
$E_0^2 b = 0{\cdot}4 \times 10^5\,\mathrm{V^2\,cm^{-1}}$ to $1 \times 10^6\,\mathrm{V^2\,cm^{-1}}$
$D_s = 0{\cdot}02$ to $0{\cdot}41$
$D_e = 0{\cdot}01$ to $0{\cdot}40$

| system no. | $\frac{D_n\,(\text{meas.})}{D_n\,(\text{calc.})^a}$ | $\frac{\phi_m\,(\text{meas.})}{\phi_m'\,(\text{calc.})^b}$ | $D_{n,B}$ (meas.) |
|---|---|---|---|
| 1 | $1{\cdot}18 \pm 0{\cdot}13$ | $1{\cdot}04 \pm 0{\cdot}40$ | $0{\cdot}26^c$ |
| 2 | $1{\cdot}02 \pm 0{\cdot}08$ | $1{\cdot}42 \pm 0{\cdot}63$ | $0{\cdot}47$ |
| 3 | $1{\cdot}03 \pm 0{\cdot}06$ | $1{\cdot}59 \pm 0{\cdot}47$ | $0{\cdot}44$ |
| 4 | $1{\cdot}00 \pm 0{\cdot}05$ | $0{\cdot}98 \pm 0{\cdot}07$ | — |
| 5 | $0{\cdot}99 \pm 0{\cdot}04$ | $1{\cdot}02 \pm 0{\cdot}06$ | $0{\cdot}43$ |
| 6 | $0{\cdot}90 \pm 0{\cdot}15$ | — | $0{\cdot}10^c$ |
| 7 | $1{\cdot}03 \pm 0{\cdot}05$ | $1{\cdot}04 \pm 0{\cdot}07$ | — |
| 9 | $0{\cdot}98 \pm 0{\cdot}07$ | $1{\cdot}03 \pm 0{\cdot}06$ | $0{\cdot}37$ |
| 13 | $1{\cdot}00 \pm 0{\cdot}05$ | $1{\cdot}06 \pm 0{\cdot}10$ | $0{\cdot}38$ |
| mean | $1{\cdot}00 \pm 0{\cdot}07$ | $1{\cdot}03 \pm 0{\cdot}07$ | $0{\cdot}42$ |

*a* From (31). *b* From (36). *c* Limiting deformation (class C).

1962*a*) drop break-up occurred from the end nearest the inner electrode as previously mentioned. The mean values of $D_{n,B}$ over the range of $G$ and $E_0$ tested given in table 4 are seen to approach the predicted values of $D_B = 0{\cdot}5$ although they are lower than the values of $D_{s,B}$ (table 2 and 3).

(2) $1 < q < \infty$. With class B materials, break-up was similar to that observed at $G = 0$ with the end nearest the negative (inner) electrode extending into a thin thread which moved along the axis of flow, with the other end then pulling out into a thread. As before when $Gb$ increased $(E_0^2 b)_B$ decreased. Also, as before, when $G$ was near $G_B$, the mode of break-up was similar to that observed for shear fields alone.

With system 1 (class C), at $Gb$ less than the limiting value, break-up occurred as in electric fields at $G = 0$. When the drop had reached the stable upper limit of deformation in the shear field (Rumscheidt & Mason 1961) the application of an electric field caused the drop to take up an orientation $\phi_m < \frac{1}{2}\pi$ and to extend from both ends into a long thread which did not break up until fluid motion was arrested. The break-up occurred by the growth of Rayleigh capillary waves (Rumscheidt & Mason 1962).

(3) $q < 1$. At low $Gb$, the mode of break-up on increasing $E_0$ was similar to that observed at $G = 0$ with the drop being squashed into a sheet which folded and twisted eventually breaking up unevenly. Just below $G_B$, increasing $E_0$ caused the drop (in class B systems) to break-up as observed with shear alone. With class C systems, at $G > G_B$, the drop deformed into a sheet which folded over without breaking up. The shape of the deformed drop in a combined shear and electric field was sometimes difficult to define; there was an apparent transition from a prolate ($E_0 = 0$) to an oblate ($G = 0$) spheroid which caused the drop to oscillate in the way observed with class C materials when a high gradient is suddenly applied (Rumscheidt & Mason 1961).

As at $G = 0$, there was a definite drift to the positive electrode in a combined shear and electric field at $q < 1$.

It is evident that in a combined shear and electric field a greater variety of modes of break-up is possible than in either field alone.

## 5. Discussion

These experiments have confirmed most of the theory outlined in § 2. Several apparent anomalies, however, remain to be explained.

(i) The principal discrepancy is the electrical deformation of certain systems into oblate spheroids, suggesting the development of an electrical stress field in which $\beta_e$ in (7) is negative instead of the predicted positive value. O'Konski & Harris calculated that this could occur as a result of modification of the fields $V_1$ and $V_2$ by electrical conduction in both phases when

$$r^2 + 7r - 2 < 6q \text{ for } r = \kappa_1/\kappa_2 > 1.$$

and

$$r^2 + 7r - 2 > 6q \text{ for } r < 1$$

Examination of the data in tables 1 and 3 shows that these conditions are not satisfied, so that this hypothesis does not apply. It may be significant that the drops appeared to acquire a net negative charge, which is ignored in the theory, but no further explanation for this interesting behaviour will be attempted here.

(ii) The values of $\gamma_e$ calculated from (17) showed good agreement with $\gamma_s$ for conducting drops, thus confirming the experimental findings of O'Konski & Gunther. In systems 1–3 and 12, $\gamma_e < \gamma_s$ suggesting that the forces acting are higher than indicated by (7). The explanation may be that since the conductivities of the drops in these cases were all considerably higher than that of the medium (see table 1), the drops behaved as if $q = \infty$. The values of $\gamma_e$ calculated from (19) for these drops are compared with $\gamma_s$ calculated from (16) in table 5. The agreement is seen to be much better than for the values of $\gamma_e$ calculated from (17).

Another possibility is that there was an accumulation of net charge on the drop because of leakage of negative charges through the silicone oil as previously discussed (Allan & Mason 1962*a*). Owing to mutual repulsion of the residual positive charges at the drop surface, an apparent decrease in interfacial tension would occur. Assuming a surface charge density $+\sigma$ uniformly distributed around

the drop, a situation which will apply strictly only at $E_0 = 0$, the apparent normal electrostatic force, $f_n'$ is

$$f_n' = \frac{2\pi\sigma^2}{K_2} = \frac{K_2 V^2}{8\pi b^2}, \tag{38}$$

where $V$ is the potential of the charged sphere at $E_0 = 0$. Laplace's equation then becomes

$$(p_i - p_0) = \frac{2\gamma}{b} - f_n' = \frac{2\gamma}{b}\left[1 - \frac{bf_n'}{2\gamma}\right] = \frac{2\gamma}{b}\left[1 - \frac{K_2 V^2}{16\pi b\gamma}\right] = \frac{2\gamma'}{b}, \tag{39}$$

where the apparent interfacial tension, $\gamma'$ is given by

$$\gamma' = \gamma - K_2 V^2/16\pi b. \tag{40}$$

Calculations from (40) showed that in systems 1, 2 and 3 ($1 < q < \infty$) a reduction in apparent surface tension of 1 dyne/cm occurs when $V = 300$ V approximately; this reduction in $\gamma$ is almost enough to account for the discrepancies and corresponds to a reasonable potential. Further experiments, however, are needed to clarify this point.

TABLE 5. $\gamma_e$ CALCULATED FROM (19) FOR SYSTEMS DEVIATING FROM (17)

$1 < q < \infty$

| system no. | $\gamma_e$[a] (dyn cm$^{-1}$) | $\gamma_s$ (dyn cm$^{-1}$) | $\gamma_e/\gamma_s$ |
|---|---|---|---|
| 1 | 2·8 | 5·6 | 0·42 |
| 2 | 4·0 | 4·3 | 0·93 |
| 3 | 2·2 | 2·8 | 0·79 |
| 12 | 6·1 | 5·8 | 1·05 |
| | | mean | 0·80 |

[a] From (19).

(iii) The measured values of $(E_0^2 b)$ and $D_{e,B}$ were much lower than those predicted by (22) and (23) in all cases as already mentioned. It must be borne in mind, however, that the theory presented above assumes that the drops remain spherical whereas, in actual fact, they deform in accordance with (17). Smythe (1953, p. 207) shows that when the surface deviates slightly from a sphere to a prolate spheroid, the surface density of the induced charge is greatly increased; this causes an increase in $f_n$ and $\beta_e$ and a decrease in $(E_0^2 b)_B$, as was found.

It would be of interest to study the break-up of the liquid threads formed in electric fields from the point of view of Tomotika's theory (1935) of the rate of growth of capillary disturbances in liquid threads as has been done for shear fields (Rumscheidt & Mason 1962).

The next paper of this series (Allan & Mason 1962*b*) deals with the corresponding behaviour of rigid conducting rods and spherical doublets.

The authors acknowledge their indebtedness to Professor R. T. Sharp of McGill University for valuable suggestions and to the Defence Research Board of Canada for financial assistance (DRB Grant 9510-05).


PROCEEDINGS OF THE ROYAL SOCIETY A MATHEMATICAL, PHYSICAL & ENGINEERING SCIENCES

## References


Allan, R. S. & Mason, S. G. 1962*a* *J. Colloid Sci.* (In the Press.)

Allan, R. S. & Mason, S. G. 1962*b* *Proc. Roy. Soc.* A, **267**, 62.

Bartok, W. & Mason, S. G. 1957 *J. Colloid Sci.* **12**, 243.

Cerf, R. 1951 *J. Chim. Phys.* **48**, 59.

Drozin, V. G. 1955 *J. Colloid Sci.* **10**, 158.

Harnwell, G. P. 1949 *Principles of electricity and magnetism*, 2nd ed. New York: McGraw-Hill Book Co. Inc.

Nawab, M. A. & Mason, S. G. 1958 *J. Colloid Sci.* **13**, 179.

O'Konski, C. T. & Gunther, R. L. 1955 *J. Colloid Sci.* **10**, 563.

O'Konski, C. T. & Harris, F. E. 1957 *J. Phys. Chem.* **61**, 1172.

O'Konski, C. T. & Thacher, H. C. 1953 *J. Phys. Chem.* **57**, 955.

Rumscheidt, F. D. & Mason, S. G. 1961 *J. Colloid Sci.* **16**, 238.

Rumscheidt, F. D. & Mason, S. G. 1962 *J. Colloid Sci.* (In the Press.)

Symthe, W. R. 1953 *Static and dynamic electricity*, 2nd ed. New York: McGraw-Hill Book Co. Inc.

Taylor, G. I. 1934 *Proc. Roy. Soc.* A, **146**, 501.

Tomotika, S. 1935 *Proc. Roy. Soc.* A, **150**, 322.

Vonnegut, B. & Neubauer, R. L. 1952 *J. Colloid Sci.* **7**, 616.

Wilson, C. T. R. & Taylor, G. I. 1925 *Proc. Camb. Phil. Soc.* **22**, 728.

Zeleny, J. 1917 *Phys. Rev.* **10** (2), 1.




PROCEEDINGS OF THE ROYAL SOCIETY A MATHEMATICAL, PHYSICAL & ENGINEERING SCIENCES